



Compensating for Soil Moisture Effects in Estimation of Soil Properties by Electrical Conductivity Sensing

Kenneth A. Sudduth, Newell R. Kitchen, Earl D. Vories, and Scott T. Drummond

USDA-ARS Cropping Systems and Water Quality Research Unit, Columbia, Missouri, USA

**A paper from the Proceedings of the
14th International Conference on Precision Agriculture
June 24 – June 27, 2018
Montreal, Quebec, Canada**

Abstract. Bulk apparent soil electrical conductivity (EC_a) is the most widely used soil sensing modality in precision agriculture. Soil EC_a relates to multiple soil properties, including clay content (i.e., texture) and salt content (i.e., salinity). However, calibrations of EC_a to soil properties are not temporally stable, due in large part to soil moisture differences between measurement dates. Therefore, the objective of this research was to investigate the effects of temporal soil moisture variations on EC_a data collected within a field with highly varying soil texture and a growing cotton crop. A variable-rate irrigation experiment imposed additional soil water content (WC) variability. Data were collected with an electromagnetic induction EC_a sensor four times within the 2017 growing season, and a fifth time pre-planting. Profile WC to approximately 68 cm depth was measured using time-domain reflectometry (TDR) sensors within season and gravimetrically pre-planting. Regressions estimating WC from EC_a data were developed and used to map spatially variable WC. Changes in EC_a -estimated WC between measurement dates corresponded reasonably well with a mapped water balance. These results are a step toward the overall goals of this research, which are to estimate WC from EC_a and also to standardize EC_a -based estimates of other soil properties for WC variation. Such standardized estimates would be beneficial, for example, to more effectively translate EC_a data into texture information that could be used for establishing variable-rate irrigation strategies.

Keywords. Soil electrical conductivity, Proximal soil sensing, Soil property estimation, Irrigation

Introduction

Soil textural variability within many irrigated fields diminishes the effectiveness of conventional irrigation management with respect to irrigation uniformity, scheduling, and water use efficiency. Irrigation scheduling methods that assume uniform soil conditions may produce less than satisfactory results on highly variable soils, contributing to a lack of commitment to irrigation scheduling by producers even though, in general, scheduling improves overall crop production.

Various approaches to spatially variable-rate irrigation (VRI) have been proposed to address this issue. Benefits of variable-rate application of agrochemicals, seeds, and nutrients can be partially masked by applying inappropriate amounts of water. However, center pivot irrigation systems can be equipped with VRI capability for site specific water application, and commercial VRI systems have been tested and shown to perform dependably (O'Shaughnessy, et al., 2013; Sui & Fisher, 2015). This logical complement to variable rate application of other inputs has producers seeking guidance for preparing prescriptions for optimal water application. Soil properties will impact the optimal irrigation rate for a given within-field location, primarily due to differences in texture leading to differences in plant available water holding capacity (AWC).

Several VRI systems primarily using soil water sensing to control application have been reported (e.g., Vellidis et al. 2008). Although technological advances have reduced cost and made arrays of multiple water content sensors more feasible, optimizing irrigation management zones to account for soil water variability remains a challenge. One approach has been to use soil apparent electrical conductivity (EC_a) surveys to map within-field texture variations at a dense spatial scale. Hedley and Yule (2009) used EC_a to map texture and AWC and then used these data in a soil water balance model to schedule irrigation. They noted that adding real-time monitoring of soil water content (WC) might provide improved results. Pan et al. (2013) used elevation and EC_a data to place WC sensors within a 37-ha field. However, VRI was not tested due to sufficient precipitation during the growing season.

Because WC is one of the main factors affecting EC_a (Rhoades et al. 1976; Kachanoski et al. 1988), it may be possible to infer temporal differences in WC directly from EC_a data. In a dryland wheat field, McCutcheon et al. (2006) found that EC_a data obtained across multiple measurement dates was strongly related to WC ($r^2 = 0.71$), while relationships to soil texture fractions were weak and often insignificant.

The goal of this research was to determine if WC could be estimated directly from multi-temporal EC_a surveys obtained within the growing season in a cotton field having highly variable soil texture. The spatially dense WC maps obtained were envisioned as a possible control input for soil moisture based VRI.

Materials and Methods

Study Field Characterization

This research was conducted at the University of Missouri Fisher Delta Research Center Marsh Farm at Portageville (36.41° N, 89.70° W) during the 2017 growing season in an irrigated cotton field. The rectangular field is approximately 5 ha, 320 m by 156 m, with the primary slope in the south to north (320 m) direction. It is located roughly 14 km west of the Mississippi River and lies within the New Madrid Seismic Zone. The combination of alluvial, eolian, and seismic activity over the years has resulted in highly variable soils in the region. While farming activities, including precision land grading, have made the effects less obvious, they still exist.

Soil mapping units within the study field included Tiptonville silt loam (fine-silty, mixed, superactive, thermic Oxyaquic Argiudolls), which made up the majority of the field, and Reelfoot loam and sandy loam (fine-silty, mixed, superactive, thermic Aquic Argiudolls) (USDA-SCS, 1971). However, the field contained areas of high sand content too small to show up in the soils map. To provide higher resolution information, mobile EC_a data were collected on 13 April 2016.

The EC_a data used in this analysis was obtained with a DUALEM 1HS instrument (Dualem, Inc., Milton, ON, Canada), which provided four channels of information that responded differently to conductivity as a function of depth (Fig. 1). These four channels were provided by two coil spacings – nominally 0.5 m and 1.0 m – along with two coil geometries – horizontal coplanar (HCP) and perpendicular (PRP) at each spacing. For convenience, the depth-response behavior of an EC_a instrument is often summarized as the depth of exploration (DOE), defined as the depth at which 70% of the cumulative response is obtained. For the channels of the 1HS instrument, the DOE varied from 0.3 to 1.6 m (Fig. 1; Dualem, 2014).

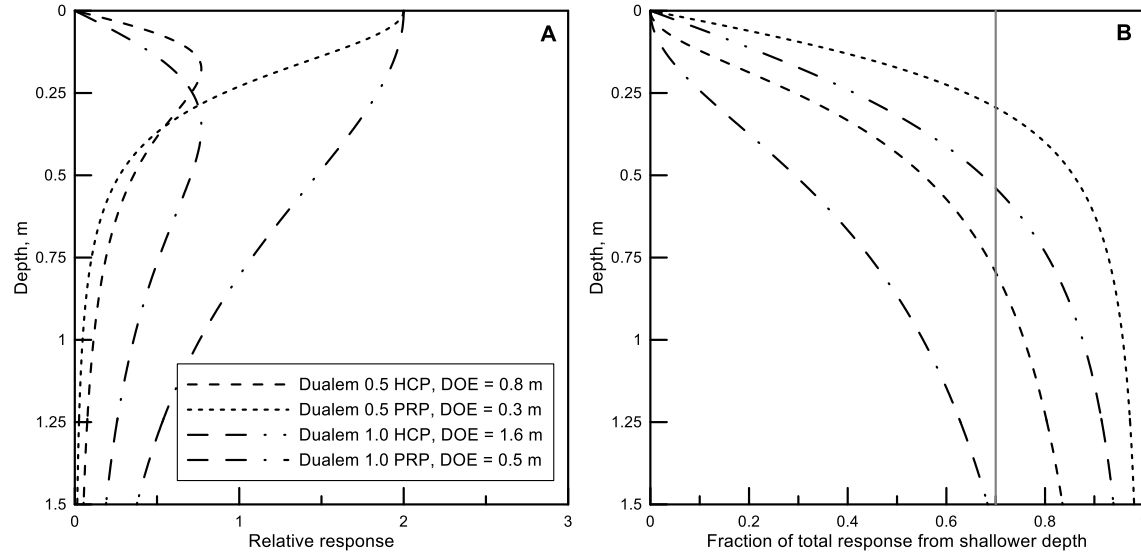


Fig 1. Incremental (A) and cumulative (B) responses of the four channels of the DUALEM 1HS EC_a sensor used in this study. Depth of exploration (DOE), defined as the depth at which 70% of the response is obtained, is shown.

Soil texture data (sand, silt, and clay fractions) from laboratory analysis were obtained by soil horizon from 8 calibration locations within the study field and an adjoining 5 ha field. These locations were chosen to cover the range in mobile EC_a data values obtained within the fields. To provide background information for this study, soil texture was estimated by calibrating profile (0-80 cm) sand and clay fractions to the 1HS EC_a data. For both sand and clay, very good fits ($r^2 \geq 0.89$) were obtained by linear regression on data from a single channel (0.5 m PRP). Maps (Fig. 2) show the high spatial variability of texture in the study field.

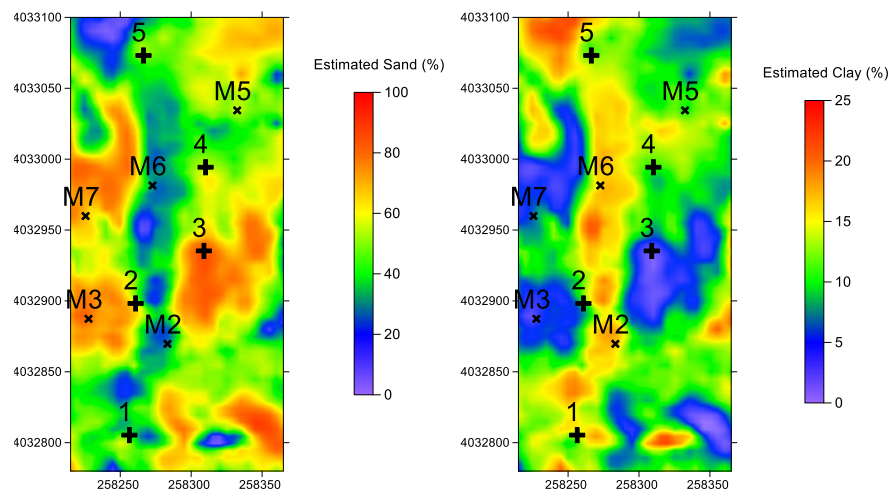


Fig. 2. Maps of EC_a-estimated profile (0-80 cm) sand and clay fractions for the study field, showing extreme variability over the 5-ha area. Points labeled M2-M7 were texture calibration core locations; points labeled 1-5 were soil moisture sensor locations (described later).

Within-Season Management and Data Collection

The field was bedded in the north-south direction with a row spacing of 0.97 m and cotton was seeded on 15 May 2017. Reduced tillage was utilized and standard cultural practices for fertilizer management and weed and insect control for producing irrigated cotton in Missouri were employed. The study field and adjoining field were irrigated using a 160 m Valley 6000 center pivot irrigation system (Valmont Irrigation, Valley, NE, USA) with a Valley Zone Control VRI system. The system included seven independently controlled zones of approximately equal area, except for the outermost zone, which consisted of the three sprinklers on the 5-m overhang beyond the outer drive tower.

The center pivot system was controlled to implement a study investigating the effects of irrigation management on cotton production (Vories et al. 2017). A rainfed treatment (R) and two irrigation treatments (A and B) were arranged in five replications, for a total of 15 sub-field areas (i.e., plots; Fig. 3). Within each of the five plots of treatment A, time-domain reflectometry (TDR) WC sensors (TDR-315, Acclima, Inc., Meridian, ID) were installed after planting at nominal 15, 30, 45, and 60 cm depths. Data were collected hourly by CR206X dataloggers (Campbell Scientific, Inc., Logan, UT) and wirelessly transmitted to a central computer.

Proximal EC_a data were collected on four dates (13 and 26 July and 4 and 11 August 2017) using the DUALEM 1HS instrument described above. A specially designed sled was used so that the 1HS could traverse the furrows between the cotton ridges while being pulled by a high-clearance vehicle (Fig. 4). Four channels of EC_a data (Fig. 1) were obtained simultaneously as described above. Data collection was terminated after 11 August when it was determined that any additional trips through the field had the potential of damaging the cotton crop due to increasing size of the cotton canopy.

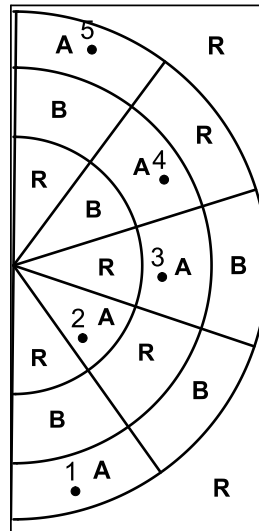


Fig. 3. Variable-rate irrigation treatment layout. R = rainfed, A & B = irrigation treatments. Points 1-5 are locations of TDR soil moisture sensors.



Fig. 4. DUALEM 1HS instrument collecting within-season EC_a data in cotton field.

Data Processing and Analysis

Data from the DUALEM 1HS surveys were “cleaned” by first adjusting for the physical distance between the instrument and the GPS, and secondly by removing a very few outliers, generally attributed to metal objects within the sensed area. When any of the channels were affected by such an anomaly, the entire data point (all channels) was removed from further analysis. Each DUALEM channel was kriged using Vesper software (University of Sydney, Australia) with appropriate semivariograms to common 1m grids. Data for the grid cells containing each calibration point (i.e., TDR or soil core location) were extracted and combined with the calibration point WC data for further analysis.

For the TDR calibration points, WC estimates from sensors installed at 15, 30, 45 and 60 cm were available at each of the survey dates in 2017, and these were included in the calibration dataset. Averaging these four readings to represent 15 cm bands created a total soil profile WC estimate over the nominal range of 7.5 to 67.5 cm. An additional calibration dataset, based on gravimetric WC, was available for the 13 April 2016 pre-plant 1HS survey described above. Coincident with the 2016 survey, soil cores were taken at eight locations in the study field, including an adjoining portion not used for this project. The samples were split into horizons, and laboratory analysis, including WC, was by horizon. A weighted average was performed on these data to also estimate profile WC over the 7.5 to 67.5 cm depth range.

Initially, only data from the in-crop surveys and corresponding TDR-based WC estimates were used to develop a calibration equation relating EC_a to soil profile WC. All four DUALEM 1HS channels (1.0 HCP, 1.0 PRP, 0.5 HCP and 0.5 PRP), along with product and quotient terms were allowed to enter into a multiple linear regression using Proc Stepwise in SAS Version 9.4 (SAS Institute, Cary, NC). However, although this model fit the data quite well, the span of measured WC was relatively low. To provide a calibration more appropriate at low WC, the gravimetric data from 2016 were included in a revised calibration.

Mapping of WC variation across the field was accomplished by applying the revised calibration to the EC_a data, kriged to a 5 m grid. Then, WC difference maps between the measurement dates were calculated from the four WC maps, allowing visualization of profile WC differences across time. For comparison with these maps, we computed a water balance for each measurement interval and for each of the 15 irrigation zones (Fig. 3) using irrigation, measured rainfall, and estimated hourly short crop evapotranspiration (ASCE-EWRI 2004) from an onsite weather station. This was only an approximate water balance, as it neglected such components as surface runoff and water movement out of the bottom of the measurement profile at 67.5 cm.

Results and Discussion

Data from each channel for all four in-crop EC_a surveys were significantly correlated (Table 1). Data from surveys closer together in time were more highly correlated, as might be expected. There was relatively little variation in any of the four EC_a channels, either within a survey date or across all dates, as shown by the low standard deviations in Table 2. Correlations among channels at a single survey date were of variable strength, with the highest correlations on the first date, and the lowest correlations on the last date. Assuming that temporal variation in EC_a is primarily attributed to changes in WC, this suggests that variability in WC as a function of depth may have increased later in the growing season. This is confirmed by TDR-measured WC (Table 3). These data show a decreasing trend in deeper (45 and 60 cm) WC data as the season progressed, however shallower (15 and 30 cm) WC data decreased to a point and then increased at the final survey date.

Table 1. EC_a correlations between initial and subsequent survey dates, by channel.

Date	Correlation vs EC _a Survey on 7/13/17			
	1.0 HCP	1.0 PRP	0.5 HCP	0.5 PRP
8/11/17	0.66	0.63	0.55	0.71
8/4/17	0.69	0.64	0.61	0.70
7/26/17	0.78	0.78	0.69	0.82

Table 2. Individual EC_a channel summary statistics for each survey date, and correlations across channels by date. Standard deviations (SD) are shown in parentheses.

Channel	Soil EC _a , mS m ⁻¹				
	7/13/17 Mean (SD)	7/26/17 Mean (SD)	8/04/17 Mean (SD)	8/11/17 Mean (SD)	All Dates Mean (SD)
1.0 HCP (A)	21.2 (2.7)	22.8 (2.6)	21.3 (1.5)	19.8 (1.6)	21.3 (2.3)
1.0 PRP (B)	17.0 (2.2)	14.5 (2.4)	15.2 (1.5)	15.2 (1.0)	15.5 (2.0)
0.5 HCP (C)	20.9 (1.2)	24.3 (1.3)	17.5 (1.2)	13.8 (1.6)	19.1 (4.2)
0.5 PRP (D)	11.7 (1.5)	9.4 (0.6)	10.7 (1.0)	11.5 (0.2)	10.8 (1.3)

Date	7/13/17	7/26/17	8/04/17	8/11/17	All Dates
A vs B	0.94	0.90	0.92	0.91	0.92
A vs C	0.89	0.95	0.95	0.95	0.78
A vs D	0.86	0.72	0.73	0.70	0.75
B vs C	0.94	0.93	0.95	0.93	0.76
B vs D	0.97	0.91	0.90	0.89	0.91
C vs D	0.89	0.80	0.82	0.77	0.52

Table 3. Measured soil moisture sensor data by depth and date. Standard deviations (SD) are shown in parentheses.

Depth (cm)	Soil Moisture (%)				
	7/13/17 Mean (SD)	7/26/17 Mean (SD)	8/04/17 Mean (SD)	8/11/17 Mean (SD)	All Dates Mean (SD)
15	13.6 (2.9)	9.8 (1.8)	9.3 (1.6)	13.5 (2.3)	11.6 (2.9)
30	19.0 (8.7)	14.2 (7.5)	12.6 (7.3)	13.4 (6.6)	14.8 (7.4)
45	30.5 (6.7)	26.5 (7.8)	22.8 (8.0)	23.0 (8.3)	25.7 (7.8)
60	32.3 (9.7)	28.2 (9.7)	25.2 (8.2)	24.1 (7.5)	27.4 (8.7)
All Depths	23.8 (4.5)	19.7 (3.8)	17.5 (4.0)	18.5 (4.3)	19.9 (4.6)

Figure 5 shows an example of EC_a and TDR data for one of the five monitoring sites. Soil WC in the surface layer was more dynamic than at the deeper layers in response to irrigation and rainfall events. Notably, the EC_a readings from the shallowest channel (0.5 PRP) also increased later in the measurement period, while readings from the deeper channels did not.

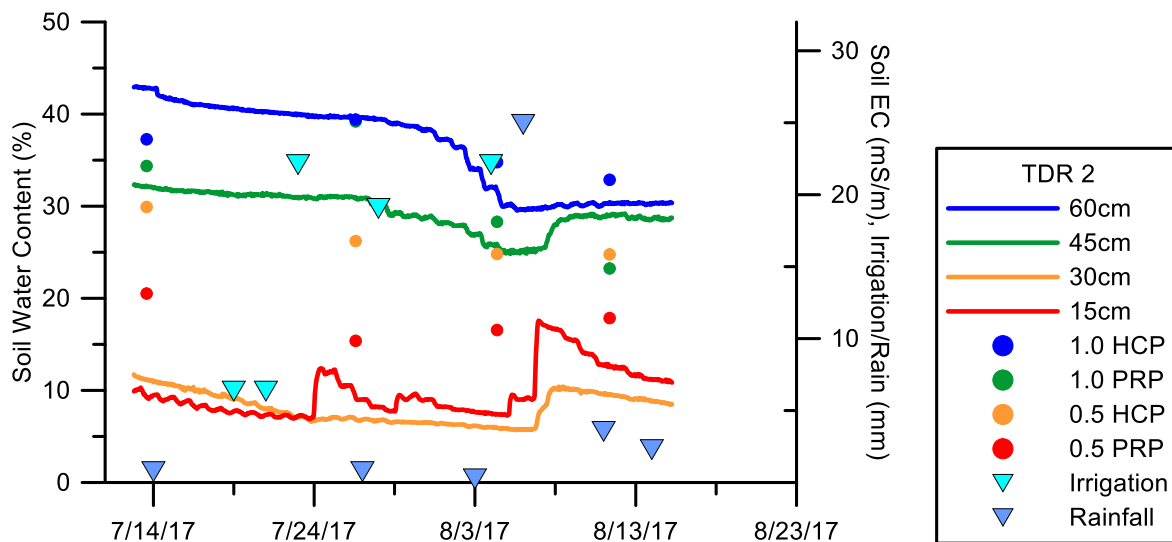


Figure 5. Variation in TDR-measured soil water content and DUALEM 1HS EC_a data over time at monitoring site 2. Rainfall and irrigation events are also shown.

Calibration of profile-average WC to EC_a data was accomplished using in-season TDR data coupled with gravimetric WC data obtained coincident with a previous EC_a survey. Good results ($R^2 = 0.79$; RMSE = 2.9%; Fig. 6) were obtained. The final model included terms based on all four DUALEM 1HS channels: 0.5 HCP, (1.0 HCP x 1.0 PRP), (1.0 HCP x 0.5 HCP), and (0.5 HCP / 0.5 PRP). Although good results were obtained for profile-average WC, attempts to develop calibrations to individual-layer WC were not successful (data not shown). The response of each of the EC_a channels to conductivity occurs over a relatively wide depth range (Fig. 1), making it difficult to separate the effects due to a defined depth layer. Approaches to calculate layer conductivities based on mathematical inversion of data from multi-channel instruments have been developed (Monteiro Santos, et al. 2010) and found to provide promising results with a different set of data collected in the study field (Sudduth et al. 2017). Use of a similar inversion approach to extract layer conductivities from this dataset is planned as part of ongoing research.

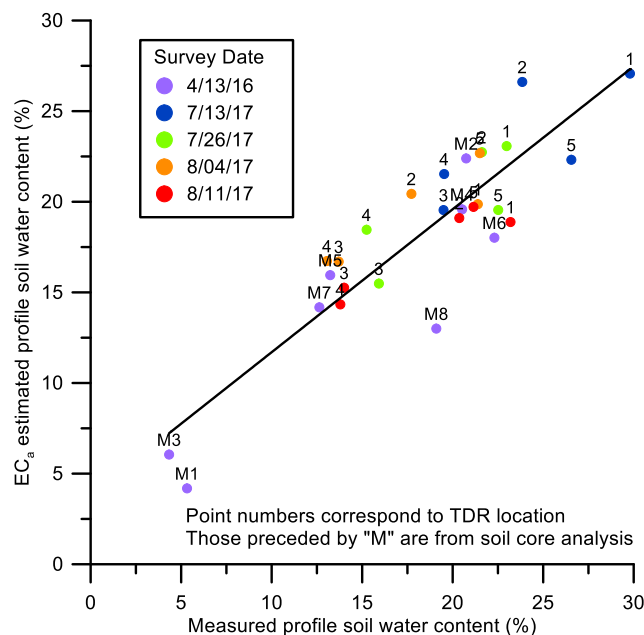


Fig. 6. Relationship of EC_a estimated profile WC to measured WC ($R^2 = 0.79$; RMSE = 2.9%).

Figure 7 shows that, in general, profile WC decreased over the 29 days between the first and last EC_a survey. The biggest decrease was in the north-south strip near the center of the field where initial WC was over 30%. Figure 2 shows this was the highest-clay portion of the field, where profile AWC would have been higher than in sandier portions of the field. The highest sand portions of the field (Fig. 2) showed the lowest WC initially and WC continued to decrease in these locations through the measurement period. Between the last two measurement dates, the change in WC was much more uniform across the field and also considerably less than in the other two increments (Fig. 7).

To better understand temporal and spatial changes in WC, we created an estimated water budget map for each of the three time increments (Fig 7). These maps were similar spatially and in level to the changes in WC mapped from successive EC_a surveys, giving a degree of confidence in the sensor-based results.

These results show that it was possible to combine point soil WC measurements (dense temporally, sparse spatially) with data from mobile EC_a surveys (sparse temporally, dense spatially) to develop a more complete understanding of spatio-temporal soil water dynamics. The good fit of profile-average WC to multi-date EC_a measurements gives confidence that it may be possible to densify point soil WC measurements using EC_a. These maps could then be useful in the development of soil-water based variable-rate irrigation strategies with higher spatial resolution.

The ability to estimate WC from EC_a might also help in standardizing EC_a measurements across different moisture levels when estimating other soil properties. If such standardization were possible, this would help facilitate combining EC_a datasets across measurement dates. Current best practices require that calibration data be obtained at each EC_a survey date so that temporal effects can be compensated. However, if temporal effects (primarily related to WC) could be effectively modeled as outlined here, that would allow more flexibility and efficiency in developing calibrations relating EC_a to other soil properties such as texture.

Conclusion

Using a combination of multi-temporal EC_a surveys and continuous point measurements of WC, it was possible to create maps of profile WC through the growing season. These maps showed that temporal variation in profile WC varied spatially throughout the field and was related to soil texture variability. Future work will attempt to enhance these results by calculating discrete layer conductivities through mathematical inversion of the EC_a signal and then using these data to create maps of how WC varies layer by layer throughout the season. The EC_a-based WC maps developed in this research provide much higher spatial resolution for soil-based irrigation scheduling than would be possible with point WC measurements alone.

Acknowledgements

We thank Kristen Veum, Kurt Holiman, and Bobby Tanner for assistance with field data collection. Mention of trade names or commercial products in this article is solely for the purpose of providing specific information and does not imply recommendation or endorsement by the U.S. Department of Agriculture.

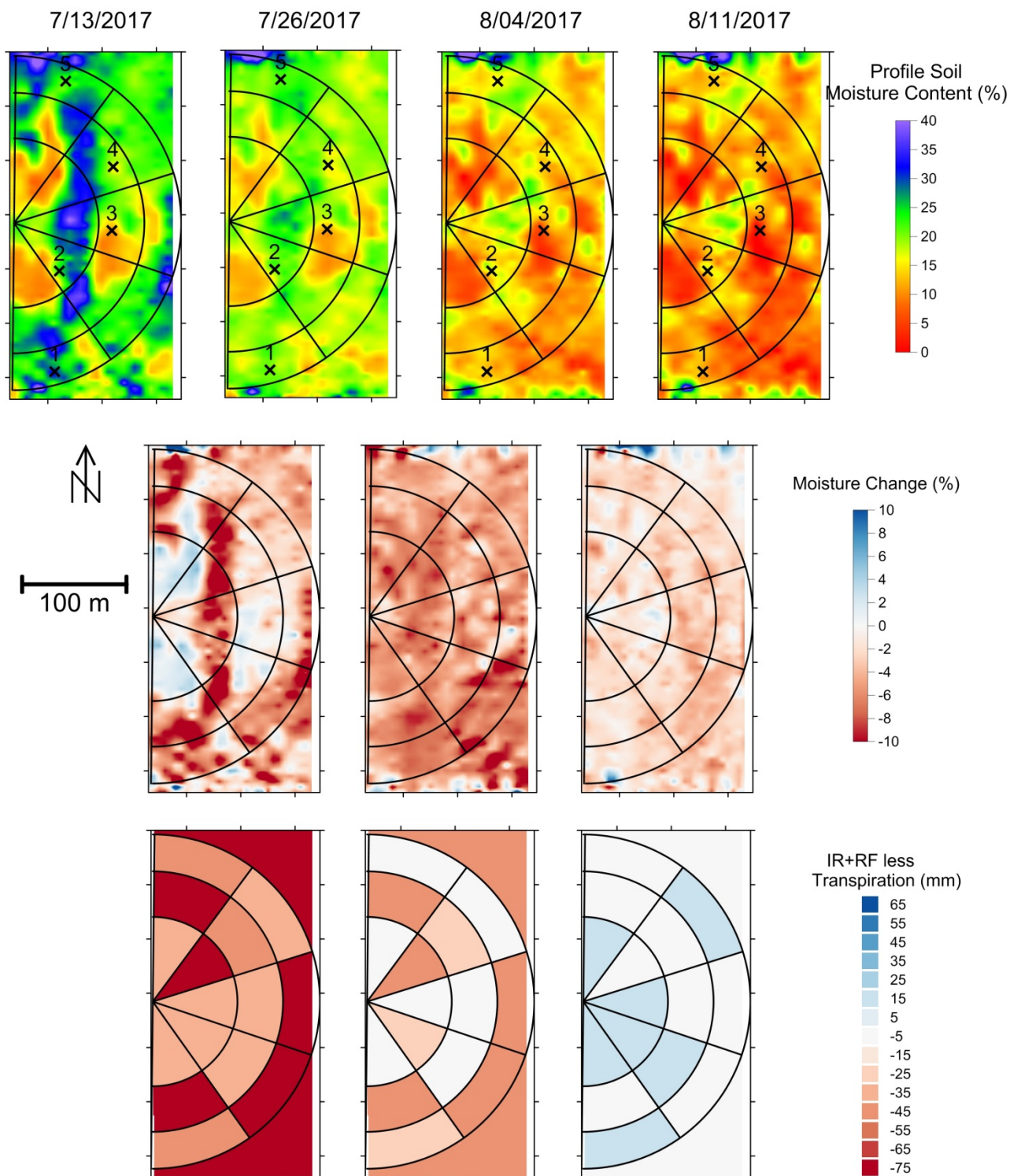


Fig. 7. Soil water (or moisture) content (WC) maps for the study field. Top: EC_a-estimated WC for each of the four survey dates. Center: Spatial change in WC in each of the three between-survey intervals. Bottom: Approximate water balance for each of the irrigation treatment areas in each of the three intervals.

References

- ASCE-EWRI. 2004. The ASCE standardized reference evapotranspiration equation. Technical Committee Report to the Environmental and Water Resources Institute of the American Society of Civil Engineers from the Task Committee on Standardization of Reference Evapotranspiration.
- Dualem (2014). DUALEM 1HS user's manual. Milton, ON, Canada: Dualem, Inc.
- Hedley, C.B. & Yule, I.J. (2009). Soil water status mapping and two variable-rate irrigation scenarios. *Precision Agriculture*, 10, 342-355.
- Kachanoski, R.G., Gregorich, E.G., & Van Wesebeeck, I.J. (1988). Estimating spatial variations of soil water content using noncontacting electromagnetic inductive methods. *Canadian Journal of Soil Science*, 68, 715-722.
- McCutcheon, M.C., Farahani, H.J., Stednick, J.D., Buchleiter, G.W., & Green, T.R. (2006). Effect of soil water on apparent soil electrical conductivity and texture relationships in a dryland field. *Biosystems Engineering*, 94(1), 19-32.
- Monteiro Santos, F. A., Triantafyllis, J., Bruzgulis, K. E. & Roe, J. A. E. (2010). Inversion of multiconfiguration electromagnetic (DUALEM-421) profiling data using a one-dimensional laterally constrained algorithm. *Vadose Zone Journal*, 9, 117-125.
- O'Shaughnessy, S. A., Urrego, Y.F., Evett, S.R., Colaizzi, P.D., & Howell, T.A. (2013). Assessing application uniformity of a variable rate irrigation system in a windy location. *Applied Engineering in Agriculture*, 29, 497-510.
- Pan, L., Adamchuk, V.I., Martin, D.L., Schroeder, M.A., & Ferguson, R.B. (2013). Analysis of soil water availability by integrating spatial and temporal sensor-based data. *Precision Agriculture*, 14, 414-433.
- Rhoades, J.D., Raats, P.A., & Prather, R.J. (1976). Effects of liquid-phase electrical conductivity, water content, and surface conductivity on bulk soil electrical conductivity. *Soil Science Society of America Journal*, 40, 651-655.
- Sudduth, K.A., Kitchen, N.R., & Drummond, S.T. (2017). Inversion of soil electrical conductivity data to estimate layered soil properties. In: Proc. 11th European Conf. on Precision Agriculture, *Advances in Animal Bioscience* 8(2): 433-438.
- Sui, R., & Fisher, D. K. (2015). Field test of a center pivot irrigation system. *Applied Engineering in Agriculture*, 31, 83-88.
- USDA-SCS (1971). Soil survey of Pemiscot County, Washington, D.C.: United States Department of Agriculture.
- Vellidis, G., Tucker, M., Perry, C., Kvien, C., & Bednarz, C. (2008). A real-time wireless smart sensor array for scheduling irrigation. *Computers and Electronics in Agriculture*, 61, 44-50.
- Vories, E.D., Sudduth, K.A., Evett, S.R., O'Shaughnessy, S.A., & Andrade, A. (2017). Comparison of crop stress and soil maps to enhance variable rate irrigation prescriptions. Paper No. 170. In: Proc 7th Asian-Australasian Conference on Precision Agriculture. <https://zenodo.org/record/893704#>. WqMDsCVG2Uk.